

Self-Organized Crystallization Patterns from Evaporating Droplets of Common Wheat Grain Leakages as a Potential Tool for Quality Analysis

Maria Olga Kokornaczyk,¹ Giovanni Dinelli,¹ Ilaria Marotti,¹ Stefano Benedettelli,² Daniele Nani,³ and Lucietta Betti¹

¹Department of Agroenvironmental Sciences and Technologies, University of Bologna, 40127 Bologna, Italy

²Department of Agronomic Science and Agro-Forestry Management, University of Firenze, 50144 Firenze, Italy

³Italian Society of Anthroposophical Medicine, 20121 Milano, Italy

Received 8 July 2011; Accepted 12 September 2011

Academic Editor: Margaret Tzaphlidou

We studied the evaporation-induced pattern formation in droplets of common wheat kernel leakages prepared out of ancient and modern wheat cultivars as a possible tool for wheat quality analysis. The experiments showed that the substances which passed into the water during the soaking of the kernels created crystalline structures with different degrees of complexity while the droplets were evaporating. The forms ranged from spots and simple structures with single ramifications, through dendrites, up to highly organized hexagonal shapes and fractal-like structures. The patterns were observed and photographed using dark field microscopy in small magnifications. The evaluation of the patterns was performed both visually and by means of the fractal dimension analysis. From the results, it can be inferred that the wheat cultivars differed in their pattern-forming capacities. Two of the analyzed wheat cultivars showed poor pattern formation, whereas another two created well-formed and complex patterns. Additionally, the wheat cultivars were analyzed for their vigor by means of the germination test and measurement of the electrical conductivity of the grain leakages. The results showed that the more vigorous cultivars also created more complex patterns, whereas the weaker cultivars created predominantly poor forms. This observation suggests a correlation between the wheat seed quality and droplet evaporation patterns.

KEYWORDS: wheat seed quality, droplet evaporation method, dark field microscopy, pattern formation, self organization, self assembly, visual evaluation, fractal dimension analysis, seed vitality

1. INTRODUCTION

The evaporation-induced formation of patterns in droplets has gained much interest during the last decade. This method is based on the phenomena of self-organization of particles suspended in fluids into nano- and microstructures during droplet evaporation and is studied by researchers working in different fields of science; it is *inter alia* important in the deposition of DNA/RNA microarrays [1–3], protein microarrays [4], DNA molecule stretching [5], drug discovery [6, 7], inkjet printing [8], and manufacture of novel electronic and optical materials [8, 9], including thin films and coatings [10]. There are also studies reporting the application of the droplet evaporation method as a diagnostic tool for medical purposes. It was possible to show that the droplets of biological fluids, such as blood serum [11–17], saliva [18], and urine [14], created different patterns depending on the patient's state of health and allowed the diagnosis of several disorders.

The evaporation of droplets of different suspensions often leads to the formation of complex patterns, like for instance patterns containing ring structures [4, 7, 19], rhythmic patterns [7, 20–23], fingering and dendrite-like patterns [24], fractals [23, 24], and hexagons [25]. The formation of patterns in evaporating droplets is still not a fully understood process. It is known that the formation and positioning of the deposit depend on the phase transition and therefore on the flow dynamics which take place during droplet evaporation. The main flow dynamics are the pinning on the contact line, which favors the particle deposition on the edge of the drop and creates the so-called coffee-ring [19, 23], the Marangoni recirculating flow driven by surface tension gradients which carries the particles toward the inside of the drop [26], and the DLVO (Derjaguin-Landau-Verwey-Overbeek) interactions, which transport the particles toward the substrate [27]. These flow dynamics influence the phase transition during the drying process of droplets and contribute thus to the pattern formation. The dynamics of these flows depend in turn on the external, environmental conditions during the evaporation and on the internal conditions inside the droplet, that is, on its composition. Among the environmental conditions known to influence the phase transition and thus the resulting pattern are temperature [7, 19, 21, 24, 26, 28], relative humidity [19, 22, 24], hydrophilicity/hydrophobicity of the substrate [7, 23, 24], pressure [1, 20, 21], and even UV radiation [29]. The composition of the liquid instead determines the droplet's characteristics, like surface tension, wettability, viscosity, ionic force, dispersion of colloids, and heat conductance [29].

However, when the drops evaporate in the same environment, their drying process depends on the liquid composition. Therefore, a slight difference in the composition of the liquid leads to changes in the phase transition during the drying process and subsequently to a different pattern [29]. This extreme sensitivity of the pattern formation processes to the liquid composition provides a wide range of possible applications of the droplet evaporation method, for instance as a tool for quality analysis of agricultural products and foods. A study performed on fresh and aged beer samples confirms this thesis and shows that the different beer samples undergo different dynamics during the evaporation processes and form therefore different patterns [30].

The idea that there is a link between the forms created through evaporation-induced pattern formation and the quality or health of the living organism is not new and has already been applied in the so-called biocrystallization or copper chloride crystallization method. This method was developed ca. a hundred years ago and consists in evaporation-induced pattern formation of a watery extract prepared out of the analyzed sample with addition of copper chloride; the features of the resulting patterns served for quality analysis of foods and agricultural products [31–33] and for diagnostic purposes in medicine [34–36]. Moreover, a standardization of the biocrystallization method as a tool for quality analysis was possible for some foods and agricultural products [31, 32].

The application of methods like droplet evaporation and biocrystallization to quality analysis requires objective techniques of pattern evaluation. In fact, pattern evaluation is often named as a weak point of these analyses [37, 38]. The most used evaluation technique is visual assessment, which has until now proved superior to computerized picture evaluation techniques [39]. However, it requires a trained panel of evaluators and is a rather time-consuming procedure. Currently, the growing arsenal of tools for fractal analysis provides new possibilities for the quantification of different and hard-to-describe features of

biological and nonbiological sets; fractal analysis seems to have a wide range of possible applications, since it has been applied in a great number of studies on images like angiograms [40, 41], ultrasound images [42], histological images [43], photographs of landscapes [44], and archeological findings [45] and on other data sets, like for instance cardiac rhythm [46].

The aim of the present study was to develop a simple method using droplet evaporation of common wheat leakages to form single spotted, fractal, and hexagon shaped-patterns on glass surfaces, and propose it for the first time as a possible method for quality analyses of common wheat. The method can be applied on whole, living seeds without the need to add any reagent; it is time-saving and fairly economic.

Moreover, in order to support our approach with traditional and easy-to-perform methods to analyze seed quality, we applied the seed vigor test by monitoring the germination rate, and the electrical conductivity of seed leakages: a fast germination with a high rate of germinated seeds, as well as low electrical conductivity of the leakage, has been found to be indicators for vigorous seeds [47–50].

2. MATERIALS AND METHODS

2.1. Wheat Samples

Four common wheat grain samples from three ancient wheat cultivars, Inallettibile (INA), Benco (BEN), and Gentil Rosso (GR), and one modern wheat cultivar, Nobel (NOB), were analyzed. Seeds from all of the investigated genotypes were grown in the same location at the experimental farm of the University of Bologna, Cadriano (latitude 44°33'N and longitude 11°21'E, 32 m a.s.l.), Italy, during the growing season 2007-2008. Until the analysis, the samples were stored at a constant temperature of 15°C and relative humidity of 12%.

2.2. Experimental Protocol for Droplet Evaporation of Wheat Leakages

For each wheat cultivar, five entire, undamaged kernels were collected and weighted. The kernels were rinsed and placed in a test tube with ultrapure water (1 : 20 w/v). The test tubes were slightly shaken by hand and left for one hour at room temperature. The experimental layout was a randomized block design with four replicates. Out of each test tube, 7 drops (3 μ L each) of leakage were collected at ca. 1 cm above the kernels and placed in one row on two 8.5 \times 9.5 cm microscope slides. The slides were previously cleaned with ethanol and thoroughly rinsed with ultrapure water.

As shown in Figure 1, 10 rows of 7 drops each were placed on each slide; the slides were then put in a thermostat at 25°C with constant UV light (UV-A Blacklight Blue Lamp, 18 W, Philips) until the end of the evaporation (approximately 1 h). Droplet residues on the slide edges (all residues in the 1st and 10th row and the 1st and 7th residue in each row) were left out because of the border effect due to different evaporation conditions, whereas the other droplet residues were used for further analysis. The experiment was repeated on four different days with a total of 320 droplet residues (4 cultivars, 5 droplet residues per cultivar replicate, 4 cultivar replicates, 4 experimentation days).

Each residue was photographed at two magnifications (25X and 100X) using a dark field microscope MT4300H, MEIJI Techno, Saitama, Japan, with a connected CMOS Camera UK1175-C, EHD imaging GmbH, Damme, Germany, in QXGA (2048 \times 1536) resolution.

2.3. Evaluation of Patterns from Droplet Residues

Images of all droplet residues in both magnifications (25X and 100X) were described for similarities and differences in their patterns. Two evaluation approaches were then developed and applied to the images: (a) visual evaluation and (b) fractal analysis.

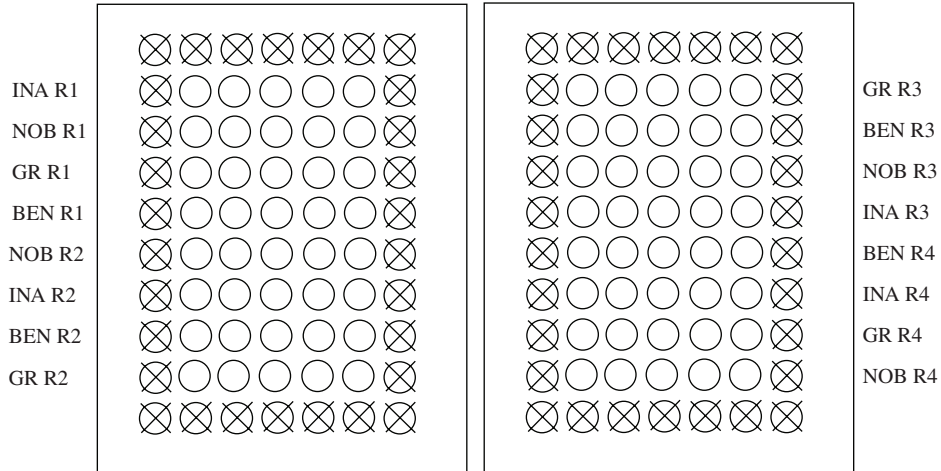


FIGURE 1: Graphical representation of the experimental design. Crossed drops were left out because of the border effect. R1–4 indicate the four replicates per cultivar.

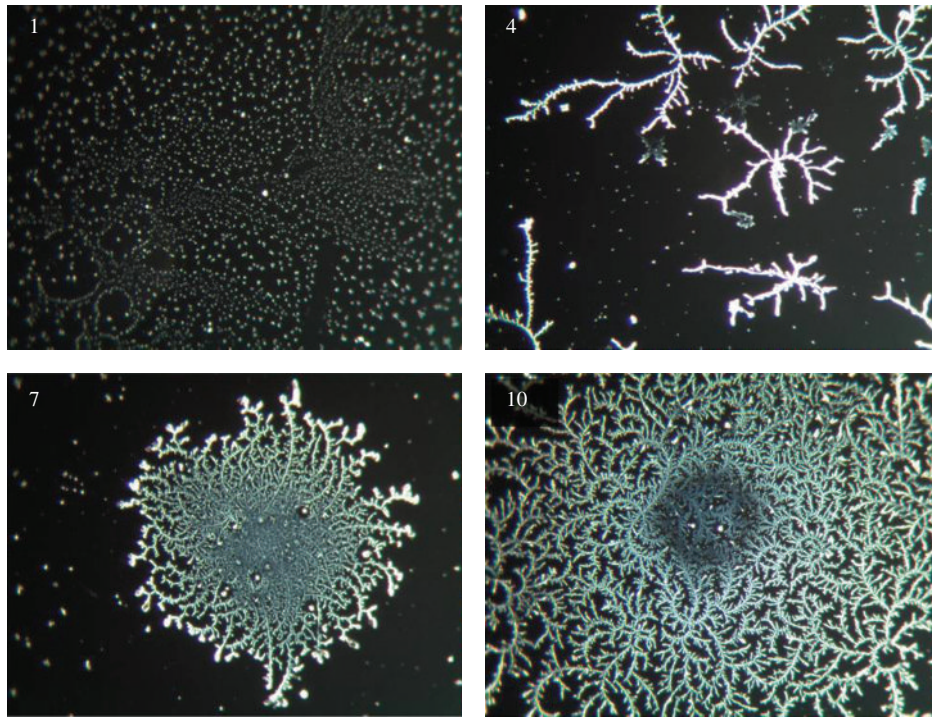


FIGURE 2: Reference pictures for visual evaluation with indication of scores (1, 4, 7, and 10), magnification 100X.

Visual Evaluation

The visual evaluation of the resulting patterns was based on a method developed for the visual evaluation of biocrystallizations described in [39] with adaptations made by our team for the evaluation of droplet patterns. The sets of images in the magnification 100X deriving from the four cultivars were letter-coded according to a blind protocol, by a person not involved in the experiment. Then, the test was performed by a nonschooled panel of 4 evaluators on an ordinal scale from 1 to 10 with reference pictures (Figure 2):

- (i) score 1 was accredited to a pattern with only single spots and/or agglomerates without any ramified structures;
- (ii) score 4 was accredited to a pattern with one or more simple ramified structures which are not grouped and do not create a centered structure;
- (iii) score 7 was accredited to a pattern with a predominant, centered, ramified structure (core), as yet rather poor in forms especially in its central part;
- (iv) score 10 was accredited to a pattern with a predominant, ramified centered structure, and very-well developed, with many wide-spreading ramifications creating ordered and complex forms.

Scores 2, 3, and 5 were accredited to the patterns showing intermediate characteristics with respect to the reference pictures if there was no centered predominant structure, and scores 6, 8, and 9 when there was a centered predominant structure.

Fractal Analysis

The fractal analysis consisted in the calculation of the local connected fractal dimension (LCFD) [40, 41] and was performed with the software *Image J for microscopy 1.43 m* [51] with the installed plugin for fractal analysis *FRAC-LAC 2.5* [52]. The images in the magnification 100X were converted to binary.

For the estimation of the LCFD, the coherent set around each pixel was used; each pixel of an object included in the coherent set of pixels was bounded by probing squares of increasing size (until 45% of the image). The fractal dimension of the D_{mass} type in the vicinity of a considered pixel was estimated from the ratio of the number of pixels to the size of the square. This procedure was repeated for all coherent pixels of an image, and the mean local dimension was then calculated. The LCFD characterized local variations of image complexity. In this analysis, any experimenter bias was avoided.

2.4. Seed Vigor Tests

The vigor of the wheat cultivars was analyzed by means of (a) germination test and (b) measurement of the electrical conductivity of seed leakages.

Germination Test

The germination test was conducted in three replicates, each consisting of 50 seeds placed in a Petri dish (120 mm diameter) containing wet sterile sand (50 g of sterile sand and 15 ml of ultrapure water). The seeds were incubated in a thermostat at 15°C in dark conditions until all shoots reached ca. 5 mm in length. The number of germinated seeds was counted daily. The experiment lasted 5 days. Based on the number of germinated seeds, the germination index (GI) was calculated as follows:

$$GI = \sum_{t=1}^n \left(\frac{G_t}{T_t} \right), \quad (2.1)$$

where G_t is the number of the germinated seeds at day t , T_t is the time corresponding to G_t in days, and n is the number of days [53].

The germination rate was expressed as the percentage of geminated seeds after five days of experimentation. The germination test was repeated twice.

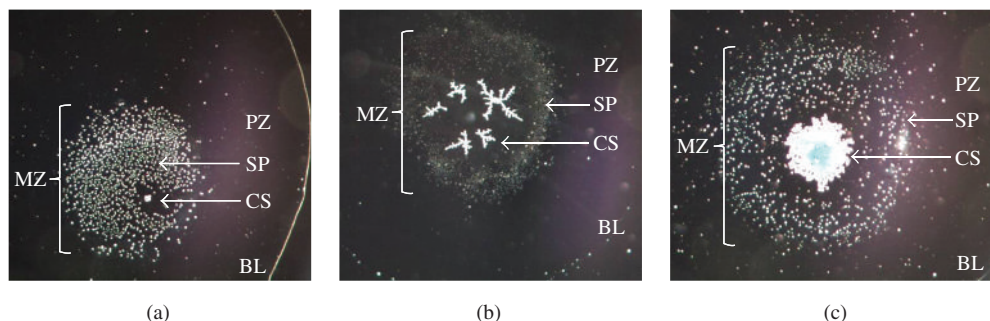


FIGURE 3: Imagines of whole droplet deposits (magnification 25X) describing crystalline structure (CS), single spot (SP), middle zone (MZ), peripheral zone (PZ), and border line (BL). Different CS shapes surrounded by several SPs are reported: (a) nonramified small CS; (b) few simple ramified and noncentered CSs; (c) complex and centered CS.

Electrical Conductivity of Seed Leakages

Two g of seeds of each wheat cultivar were washed and then soaked in 40 mL of ultrapure water at room temperature. Electrical conductivity of seed leakages was measured after 24 h of soaking (time necessary for pointing out the differences in electrical conductivity of seed leakages from different cultivars) using a conductivity meter (Basic 30, CRISON Instruments S.A., Barcelona, Spain) and expressed as $\mu\text{S cm}^{-1}$ [49]. The experiment was replicated four times.

2.5. Statistical Analysis

All data was analyzed by means of the Bartlett test and analysis of variance (CoStat, version 6.400). Multiple mean comparison was carried out by Turkey's HSD test.

In addition, the Bravais-Pearson linear coefficient of correlation $r = (\text{Cov}(X, Y))/(\text{SD}(X)\text{SD}(Y))$ was computed to determine the degree of association between the data of visual evaluation and fractal analysis.

3. RESULTS AND DISCUSSION

3.1. General Description of Patterns from Droplet Residues

All droplet patterns consisted of a prevalent deposition in the middle zone and of a thin and rather small visible border line, whereas the peripheral zone, that is, the space between the middle zone and the border line, was structure-free (Figure 3(a)). The deposition in the middle zone consisted of one or a few crystalline structures (CSs) surrounded by single spots (Figures 3(a)–3(c)). The CSs were composed of connected deposits of varying sizes and complexity, usually located in the middle zone of the evaporated droplets (Figures 3(a)–3(c)). In the middle zone, the subdivision of the deposit into connected CSs and single spots suggested the spatial segregation of substances during the evaporation process. Spatial segregation in evaporating droplets has been reported for suspensions of different sized nanoparticles [28], nanospheres [54] and for complex fluids [55].

The CS was the main variable pattern element among the droplet deposits: shapes ranged from single spots and crosses (Figures 4(a) and 4(b)), through dendrites (Figures 4(c) and 4(d)), up to complex (Figures 4(e)–4(i)) and highly organized structures (Figures 4(j)–4(l)). The CSs consisted mainly of ramified branches (Figures 4(a)–4(f) and 4(j)–4(l)) and, in some cases, also of amorphous agglomerations placed in their central parts (Figures 4(g) and 4(h)). As regards CS ramifications, different shapes of branches were

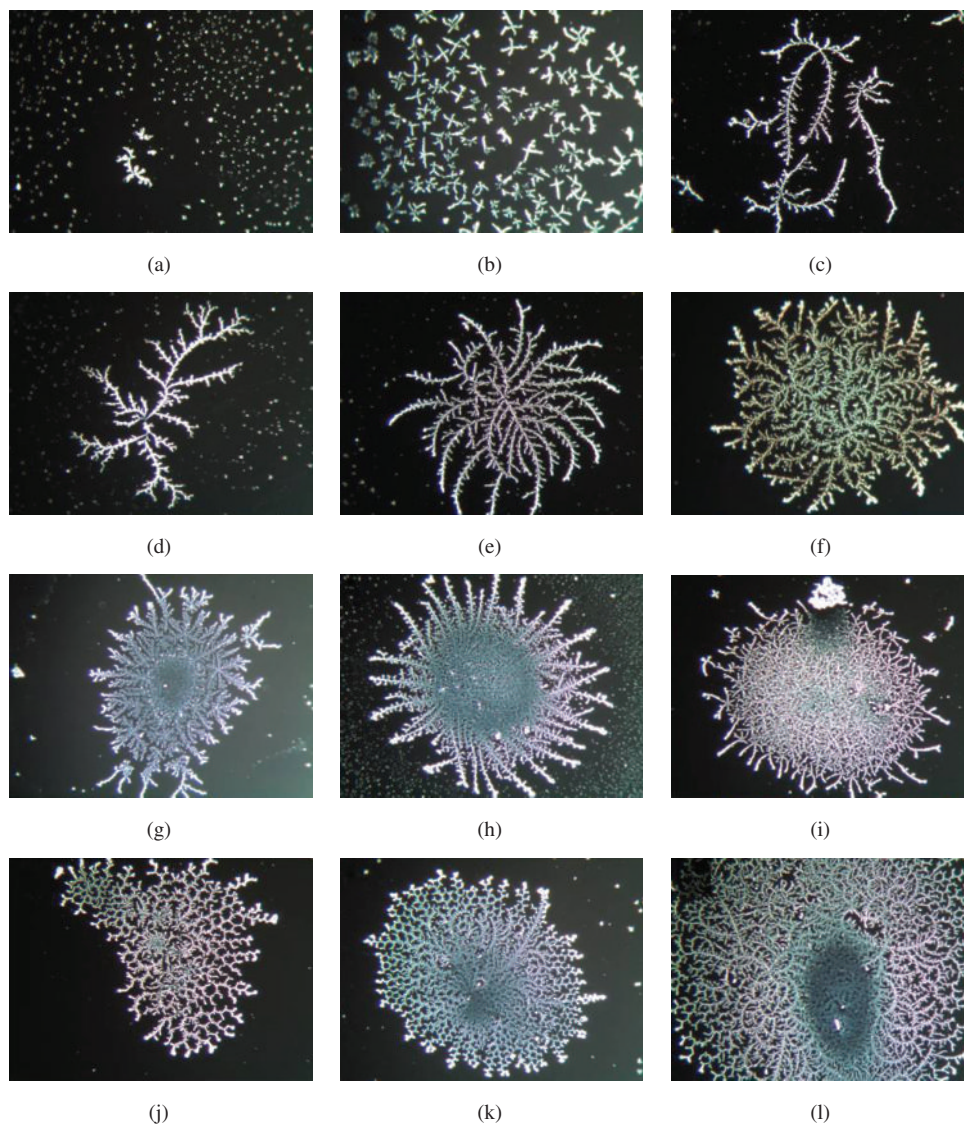


FIGURE 4: Examples of crystalline structures showing different degrees of complexity (magnification 100X): single spots and crosses (a, b), dendrites (c, d), ramified complex structures (e, f), structures containing agglomerates (g, h), complex structures with short disordered ramifications (i), high organized fractal-like structures containing hexagons (j, k), and curled branches (l).

observed: straight (Figure 4(h)), curved (Figure 4(e)), curled (Figures 4(f) and 4(l)), or hexagonal (Figures 4(j) and 4(k)).

The formation of ramified branched structures in evaporating droplets can be explained by the diffusion limited aggregation due to Brownian motion of particles [24]: several CSs obtained in the present research (Figure 4(d)) showed a great similarity to Brownian trees [56]. In addition, hexagonal shapes were found in evaporating droplets containing nanoparticles [27] and nanospheres [54] and were detected in many different auto-organizing systems, as for instance the cells in Rayleigh-Bénard convection [57]. Dendritic and hexagonal shapes have been observed in evaporating droplets from different suspensions suggesting that these structures seem to be a common feature of self-organizing systems rather than strictly dependant on solute/solvent molecular characteristics [58].

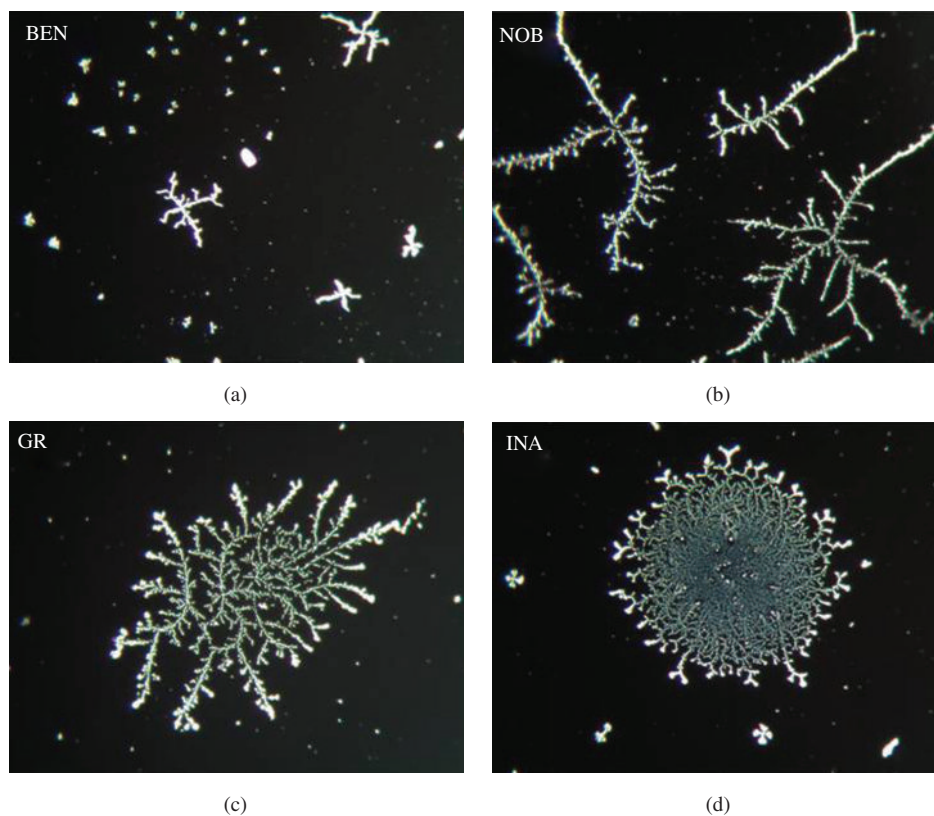


FIGURE 5: Examples of images scored in the visual evaluation by values 3, 4, 6, and 7 for the wheat cultivars Benco (BEN), Nobel (NOB), Gentil Rosso (GR), and Inallettibile (INA), respectively, (magnification 100X).

TABLE 1: Visual assessment of images from different wheat cultivars: mean score, coefficient of variation (CV), and percentage of patterns with a single crystallization core (Patterns_{SC}). Different letters indicate significant differences at $P < 0.05$.

Cultivar	<i>N</i>	Mean score	SE	CV (%)	Patterns _{SC} (%)
Inallettibile	80	6.98 (a)	0.23	30	76
Gentil Rosso	80	6.08 (a)	0.26	38	65
Nobel	80	3.81 (b)	0.26	60	26
Benco	80	3.32 (b)	0.22	59	17

N: number of evaluated patterns; SE: standard error.

3.2. Evaluation of Image Patterns

Visual Evaluation

The visual assessment, carried out by four independent evaluators on 80 images for each wheat cultivar, revealed different levels of complexity within the experimental data set (Table 1). Inallettibile and Gentil Rosso showed significantly higher mean scores indicating a more complex CS organization than Nobel and Benco (Figure 5). In addition, a great proportion, ranging from 76 to 65%, of Inallettibile and Gentil Rosso patterns was characterized by a single prevalent crystallization core, while Nobel and Benco showed predominantly patterns with multiple crystallization cores.

TABLE 2: Mean values of the local connected fractal dimension (LCFD) analysis of the images from the four analyzed wheat cultivars. Different letters indicate significant differences at $P < 0.05$.

Cultivar	N	LCFD	
		Mean	SE
Inallettabile	80	1.340 (a)	0.030
Gentil Rosso	80	1.214 (a)	0.039
Nobel	80	1.006 (b)	0.039
Benco	80	0.885 (b)	0.038

N: number of evaluated patterns; SE: standard error.

In visual assessment, two main sources of variation have to be considered: the first one is the variability due to different self-assembling shapes within each genotype; the second one is related to the different evaluation of the same image among the evaluators. As shown by coefficient of variation values, the mean score variability for Inallettabile and Gentil Rosso was approximately half that of Nobel and Benco (Table 1). The lower coefficients of variation were associated with Inallettabile and Gentil Rosso, which produced a predominance of patterns characterized by a single crystallization core. These data suggest a more homogeneous scoring for highly organized patterns. The opposite was observed for Nobel and Benco, which predominantly created patterns with multiple crystallization cores and more prone to divergent assessment among evaluators.

Computer-Assisted Evaluation: Fractal Analysis

The mean values of the local connected fractal dimension (LCFD) are shown in Table 2. The analysis showed that the cultivars Inallettabile and Gentil Rosso differed significantly from Nobel and Benco: Inallettabile and Gentil Rosso had higher LCFD values indicating a greater complexity of the CSs.

Figure 6 depicts the correlations between the data gained in the two applied pattern evaluation approaches: visual evaluation and fractal analysis (LCFD) for each of the given wheat cultivar. The data sets were positively correlated ($r = 0.72$), at $P < 0.001$. This shows that the two evaluation approaches had the same trend and that the visual approach was comparable with an objective assessment such as the fractal analysis.

In our study, the evaporation process was conducted at 25°C and constant UV light. These conditions (room temperature and UV lightening) were reported in some studies [29] as appropriate, and also in our experiments they turned out to be suitable for the here described analysis. However, an improved control of the evaporating conditions including relative humidity and pressure might increase the method's repeatability and robustness. Another step, which may be considered for further improvements, is the collection of droplets from the wheat seed leakages. In the present study, we collected each droplet by immersing a micropipette into the leakage to the depth of ca. 1 cm above the kernels. This procedure however provokes flows in the remaining leakage and may cause variations between droplets collected from the same tube and in consequence in pattern repetitions.

3.3. Seed Vigor Tests

The germination index, germination rate, and electrical conductivity of seed leakages indicated that the cultivars Inallettabile and Gentil Rosso were significantly more vigorous than the cultivars Nobel and Benco (Table 3). They germinated faster and had a higher germination rate, and the electrical conductivity of the seed leakage was lower.

It is worth noting that the analyzed cultivars showed an interesting alignment of the results coming from both kinds of analysis: the droplet evaporation method and vigor test. The cultivars which created

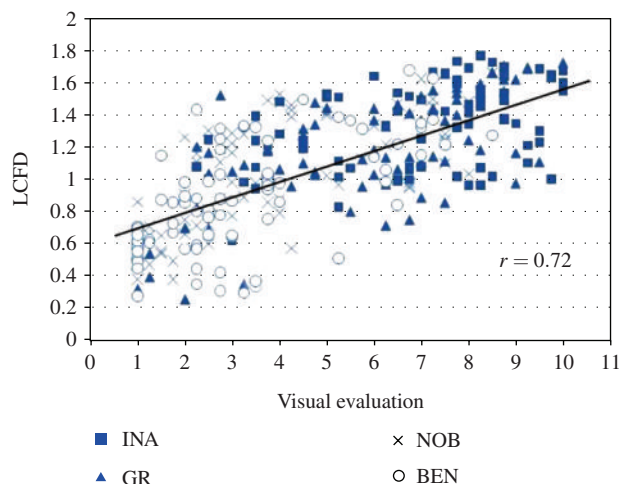


FIGURE 6: Correlation of data sets derived from the both evaluation approaches: visual evaluation and the local connected fractal dimension (LCFD). The wheat cultivars Inallettabile (INA), Gentil Rosso (GR), Nobel (NOB), and Benco (BEN) are signed by different indicator shapes.

TABLE 3: Results of the seed vigor tests. Data are presented as mean values. Different letters indicate significant differences at $P < 0.05$.

Cultivar	N	Germination index		Germination rate (%)		Electrical conductivity ($\mu\text{S cm}^{-1}$)		
		Mean	SE	Mean	SE	N	Mean	SE
Inallettabile	6	24.30 (ab)	0.45	94.70 (a)	1.80	4	101.20 (a)	3.03
Gentil Rosso	6	26.47 (a)	1.42	95.30 (a)	0.67	4	108.10 (ab)	5.66
Nobel	6	18.97 (c)	1.90	77.00 (b)	1.36	4	125.90 (c)	4.04
Benco	6	20.77 (bc)	1.05	87.70 (b)	1.17	4	119.10 (bc)	4.23

N: number of samples; SE: standard error.

large and complex CS (Inallettabile and Gentil Rosso) proved to be more vital, whereas the cultivars Nobel and Benco, which created smaller or no CS and had a low percentage of one cored patterns (Table 1) also showed poor vitality in the applied seed vigor test. These findings suggest that the pattern complexity might reflect the seed vitality; they conform also to the overall experience gained in various studies using different methods based on pattern formation, which showed that, generally, a better vitality or health proved to be associated with patterns showing greater complexity, rich forms, and greater harmony [39, 59, 60].

4. CONCLUSIONS

We have shown that, while evaporating, droplets of wheat seed leakages create patterns containing a wide range of differently shaped crystalline structures. In our experiment, we analyzed droplet patterns prepared from four different wheat cultivars. The evaluation of these patterns was carried out by means of visual evaluation and fractal dimension analysis; the data deriving from both applied evaluation approaches showed a strong correlation. It was possible to show that the analyzed wheat cultivars differed in the complexity of their droplet patterns. Furthermore, the results of the vigor test revealed that the pattern complexity corresponded with the vitality of the seeds.

These results seem to be highly encouraging for considering the droplet evaporation method of wheat seed leakages as a possible tool for quality and vitality analysis of wheat. Furthermore, by introducing appropriate modifications to the experimental protocol, this method might represent also an appropriate

quality analysis tool for other agricultural seeds and products. However, a solid basic research is of great importance because primarily the understanding of self-assembly underlying mechanisms will permit the diffusion of the droplet evaporation method, as well as other crystallization methods, as tools for quality analysis. This study certainly represents only the beginning, and further research and collaboration of different fields of science is indispensable for the better understanding of the approach to quality presented here.

ACKNOWLEDGMENTS

The authors would like to thank Demeter Italy and the Biodynamic Association Italy for funding this research. Particular acknowledgement goes to Dr. Antonello Russo for his precious support and to Dr. Edda Sanesi for her encouragement. The authors also thank Weleda Italia for financial support in the publication costs. Finally, a special thanks goes to Dr. Inge Just-Nastansky and Professor Bernd Kroepelin for their scientific advice and to Professor Ida Domini for her pertinent observations and discussions.

REFERENCES

- [1] V. Dugas, J. Broutin, and E. Souteyrand, “Droplet evaporation study applied to DNA chip manufacturing,” *Langmuir*, vol. 21, no. 20, pp. 9130–9136, 2005.
- [2] J. Jing, J. Reed, J. Huang et al., “Automated high resolution optical mapping using arrayed, fluid-fixed DNA molecules,” *Proceedings of the National Academy of Sciences of the United States of America*, vol. 95, no. 14, pp. 8046–8051, 1998.
- [3] M. Schena, D. Shalon, R. Heller, A. Chai, P. O. Brown, and R. W. Davis, “Parallel human genome analysis: microarray-based expression monitoring of 1000 genes,” *Proceedings of the National Academy of Sciences of the United States of America*, vol. 93, no. 20, pp. 10614–10619, 1996.
- [4] Y. Deng, X. Y. Zhu, T. Kienlen, and A. Guo, “Transport at the air/water interface is the reason for rings in protein microarrays,” *Journal of the American Chemical Society*, vol. 128, no. 9, pp. 2768–2769, 2006.
- [5] I. I. Smalyukh, O. V. Zribi, J. C. Butler, O. D. Lavrentovich, and G. C. L. Wong, “Structure and dynamics of liquid crystalline pattern formation in drying droplets of DNA,” *Physical Review Letters*, vol. 96, no. 17, Article ID 177801, 2006.
- [6] G. Arrabito and B. Pignataro, “Inkjet printing methodologies for drug screening,” *Analytical Chemistry*, vol. 82, no. 8, pp. 3104–3107, 2010.
- [7] P. Takhistov and H. C. Chang, “Complex stain morphologies,” *Industrial and Engineering Chemistry Research*, vol. 41, no. 25, pp. 6256–6269, 2002.
- [8] W. R. Small, C. D. Walton, J. Loos, and M. In Het Panhuis, “Carbon nanotube network formation from evaporating sessile drops,” *Journal of Physical Chemistry B*, vol. 110, no. 26, pp. 13029–13036, 2006.
- [9] T. Kawase, H. Sirringhaus, R. H. Friend, and T. Shimoda, “Inkjet printed via-hole interconnections and resistors for all-polymer transistor circuits,” *Advanced Materials*, vol. 13, no. 21, pp. 1601–1605, 2001.
- [10] N. Chakrapani, B. Wei, A. Carrillo, P. M. Ajayan, and R. S. Kane, “Capillarity-driven assembly of two-dimensional cellular carbon nanotube foams,” *Proceedings of the National Academy of Sciences of the United States of America*, vol. 101, no. 12, pp. 4009–4012, 2004.
- [11] K. Sefiane, “On the formation of regular patterns from drying droplets and their potential use for bio-medical applications,” *Journal of Bionic Engineering*, vol. 7, supplement, pp. S82–S93, 2010.
- [12] Y. Yakhno, “Protein phase instability development in plasma of sick patients: clinical observations and model experiments,” *Natural Science*, vol. 2, pp. 220–227, 200.
- [13] A. K. Martusevich, Y. Zimin, and A. Bochkareva, “Morphology of dried blood serum specimens of viral hepatitis,” *Journal of Hepatitis Monthly*, vol. 7, pp. 207–210, 2007.
- [14] A. K. Martusevich and N. F. Kamakin, “Crystallography of biological fluid as a method for evaluating its physicochemical characteristics,” *Bulletin of Experimental Biology and Medicine*, vol. 143, no. 3, pp. 385–388, 2007.

- [15] A. A. Killeen, N. Ossina, R. C. McGlennen et al., “Protein self-organization patterns in dried serum reveal changes in B-cell disorders,” *Molecular Diagnosis and Therapy*, vol. 10, no. 6, pp. 371–380, 2006.
- [16] T. A. Yakhno, O. A. Sedova, A. G. Sanin, and A. S. Pelyushenko, “On the existence of regular structures in liquid human blood serum (plasma) and phase transitions in the course of its drying,” *Technical Physics*, vol. 48, no. 4, pp. 399–403, 2003.
- [17] E. Rapis, “A change in the physical state of a nonequilibrium blood plasma protein film in patients with carcinoma,” *Technical Physics*, vol. 47, no. 4, pp. 510–512, 2002.
- [18] A. B. Denisov, “Algorithm for evaluation of crystal figures obtained after drying of mixed saliva,” *Bulletin of Experimental Biology and Medicine*, vol. 138, no. 1, pp. 30–33, 2004.
- [19] R. D. Deegan, O. Bakajin, T. F. Dupont, G. Huber, S. R. Nagel, and T. A. Witten, “Contact line deposits in an evaporating drop,” *Physical Review E*, vol. 62, no. 1, pp. 756–765, 2000.
- [20] G. Chen and G. J. Mohamed, “Complex protein patterns formation via salt-induced self-assembly and droplet evaporation,” *European Physical Journal E*, vol. 33, no. 1, pp. 19–26, 2010.
- [21] D. Kaya, V. A. Belyi, and M. Muthukumar, “Pattern formation in drying droplets of polyelectrolyte and salt,” *Journal of Chemical Physics*, vol. 133, no. 11, Article ID 114905, 2010.
- [22] R. G. Gary Larson, M. Alumnà López, D. W. Lim, and J. Lahann, Complex Protein Patterns in Drying Droplets. MRS Proceedings, 1273, 1273-MM03-0, 2010.
- [23] R. D. Deegan, “Pattern formation in drying drops,” *Physical Review E*, vol. 61, no. 1, pp. 475–485, 2000.
- [24] J. Zhang, S. K. Kim, X. Sun, and H. Lee, “Ramified fractal-patterns formed by droplet evaporation of a solution containing single-walled carbon nanotubes,” *Colloids and Surfaces A*, vol. 292, no. 2-3, pp. 148–152, 2007.
- [25] K. Mougin and H. Haidara, “Complex pattern formation in drying dispersions,” *Langmuir*, vol. 18, no. 24, pp. 9566–9569, 2002.
- [26] H. Hu and R. G. Larson, “Marangoni effect reverses coffee-ring depositions,” *Journal of Physical Chemistry B*, vol. 110, no. 14, pp. 7090–7094, 2006.
- [27] R. Bhardwaj, X. Fang, P. Somasundaran, and D. Attinger, “Self-assembly of colloidal particles from evaporating droplets: role of DLVO interactions and proposition of a phase diagram,” *Langmuir*, vol. 26, no. 11, pp. 7833–7842, 2010.
- [28] H. C. Chon, S. Paik, J. B. Tipton, and K. D. Kihm, “Effect of nanoparticle sizes and number densities on the evaporation and dryout characteristics for strongly pinned nanofluid droplets,” *Langmuir*, vol. 23, no. 6, pp. 2953–2960, 2007.
- [29] T. Yakhno, V. Yakhno, A. Sanin, O. Sanina, and A. Pelyushenko, “Dynamics of phase transitions in drying drops as an information parameter of liquid structure,” *Nonlinear Dynamics*, vol. 39, no. 4, pp. 369–374, 2005.
- [30] T. A. Yakhno, V. G. Yakhno, A. G. Sanin, O. A. Sanina, and A. S. Pelyushenko, “A method for liquid analysis by means of recording the dynamics of phase transition during drop drying,” in *Bioengineered and Bioinspired Systems Conference*, vol. 5119 of *Proceedings of SPIE*, Gran Canaria, Spain, May 2003.
- [31] N. Busscher, J. Kahl, J. O. Andersen et al., “Standardization of the biocrystallization method for carrot samples,” *Biological Agriculture and Horticulture*, vol. 27, pp. 1–23, 2010.
- [32] J. Kahl, N. Busscher, P. Doesburg, G. Mergardt, M. Huber, and A. Ploeger, “First tests of standardized biocrystallization on milk and milk products,” *European Food Research and Technology*, vol. 229, no. 1, pp. 175–178, 2009.
- [33] M. Kokornaczyk, J. Kahl, M. Roose, N. Busscher, and A. Ploeger, “Organic wheat quality from a defined Italian field-trial. Cultivating the Future Based on Science,” in *Proceedings of the 2nd Conference of the International Society of Organic Agriculture Research (ISO FAR '08)*, vol. 2, pp. 746–749, Modena, Italy, June 2008.
- [34] T. Shibata, S. Matsumoto, M. Kogure et al., “Effects of diabetic human blood addition on morphology of cupric chloride dendrites grown from aqueous solutions,” *Journal of Crystal Growth*, vol. 219, no. 4, pp. 423–433, 2000.
- [35] T. Shibata, Y. Takakuwa, A. Tanaka, T. Iguchi, M. Kogure, and T. Ogawa, “Doping effect of human blood on surface microstructure of cupric chloride dendrites grown from aqueous solutions,” *Journal of Crystal Growth*, vol. 167, no. 3-4, pp. 716–718, 1996.
- [36] T. Shibata, R. Shirasaka, T. Ogawa et al., “Effect of human blood addition on dendritic growth of cupric chloride crystals in aqueous solutions,” *Journal of Crystal Growth*, vol. 142, no. 1-2, pp. 147–155, 1994.
- [37] S. Heaton, *Organic Farming, Food Quality and Human Health—A Review of the Evidence*, Soil Association, Bristol, UK, 2001.

- [38] K. Woese, D. Lange, C. Boess, and K. W. Bögl, “A comparison of organically and conventionally grown foods—results of a review of the relevant literature,” *Journal of the Science of Food and Agriculture*, vol. 74, no. 3, pp. 281–293, 1997.
- [39] M. Huber, J. O. Andersen, J. Kahl et al., “Standardization and validation of the visual evaluation of biocrystallisations,” *Biological Agriculture and Horticulture*, vol. 27, pp. 25–40, 2010.
- [40] H. F. Jelinek, D. J. Cornforth, A. J. Roberts, G. Landini, P. Bourke, and A. Iorio, “Image processing of finite size rat retinal ganglion cells using multifractal and local connected fractal analysis,” in *Advances in Artificial Intelligence: 17th Australian Joint Conference on Artificial Intelligence*, G. I. Webb and X. Yu, Eds., vol. LNAI 3339, pp. 961–966, Springer, December 2004.
- [41] G. Landini, P. I. Murray, and G. P. Misson, “Local connected fractal dimensions and lacunarity analyses of 60° fluorescein angiograms,” *Investigative Ophthalmology and Visual Science*, vol. 36, no. 13, pp. 2749–2755, 1995.
- [42] D. R. Chen, R. F. Chang, C. J. Chen et al., “Classification of breast ultrasound images using fractal feature,” *Clinical Imaging*, vol. 29, no. 4, pp. 235–245, 2005.
- [43] R. A. Eid and G. Landini, “The complexity of oral mucosa: a review of the use of fractal geometry,” *C.E.A.I.*, vol. 12, no. 1, pp. 10–14, 2010.
- [44] W. M. Hern, “Urban malignancy: similarity in the fractal dimensions of urban morphology and malignant neoplasm,” *International Journal of Sociology and Anthropology*, vol. 23, no. 1-2, pp. 1–19, 2008.
- [45] C. T. Brown and W. R. T. Witschey, “The fractal geometry of ancient Maya settlement,” *Journal of Archaeological Science*, vol. 30, no. 12, pp. 1619–1632, 2003.
- [46] M. Saeed, “Fractals analysis of cardiac arrhythmias,” *TheScientificWorldJournal*, vol. 5, pp. 691–701, 2005.
- [47] A. Ali, S. U. Siddiqui, M. Afzal, and M. F. Chaudhary, “Response of wheat (*Triticum aestivum* L.) var. Chakwal-97 to artificial ageing in relation to its viability under mid-term conservation in genebank,” *Pakistan Journal of Botany*, vol. 38, no. 4, pp. 1071–1078, 2006.
- [48] S. M. A. Basra, I. Afzal, R. A. Rashid, and M. Farooq, “Pre-sowing seed treatments to improve germination and seedling growth in wheat (*Triticum aestivum* L.),” *Caderno de Pesquisa Serie Biologia*, vol. 17, no. 1, pp. 155–164, 2005.
- [49] S. M. A. Basra, I. A. Pannu, and I. Afzal, “Evaluation of seedling vigor of hydro and matriprimed wheat (*Triticum aestivum* L.) seeds,” *International Journal of Agriculture and Biology*, vol. 5, no. 2, pp. 121–123, 2003.
- [50] M. Tajbakhsh, “Relationships between electrical conductivity of imbibed seeds leachate and subsequent seedling growth (viability and vigour) in Omid wheat,” *Journal of Agriculture, Science and Technology*, vol. 2, pp. 67–71, 2000.
- [51] T. J. Collins, “ImageJ for microscopy,” *BioTechniques*, vol. 43, no. 1, pp. 25–30, 2007.
- [52] A. Karperien, (1999–2007) FracLac for ImageJ, version 2.5, <http://rsb.info.nih.gov/ij/plugins/fraclac/FLHelp/Introduction.htm>.
- [53] D. D. Cao, J. Hu, X. X. Huang, X. J. Wang, Y. J. Guan, and Z. F. Wang, “Relationships between changes of kernel nutritive components and seed vigor during development stages of F1 seeds of sh2 sweet corn,” *Journal of Zhejiang University*, vol. 9, no. 12, pp. 964–968, 2008.
- [54] A. P. Sommer, M. Ben-Moshe, and S. Magdassi, “Size-discriminative self-assembly of nanospheres in evaporating drops,” *Journal of Physical Chemistry B*, vol. 108, no. 1, pp. 8–10, 2004.
- [55] Y. Y. Tarasevich and D. M. Pravoslavnova, “Segregation in desiccated sessile drops of biological fluids,” *European Physical Journal E*, vol. 22, no. 4, pp. 311–314, 2007.
- [56] J. Pitman and M. Winkel, “Growth of the brownian forest,” *Annals of Probability*, vol. 33, no. 6, pp. 2188–2211, 2005.
- [57] U. Thiele and K. Eckert, “Stochastic geometry of polygonal networks: an alternative approach to the hexagon-square transition in Bénard convection,” *Physical Review E*, vol. 58, no. 3, pp. 3458–3468, 1998.
- [58] A. Sukhanova, Y. Volkov, A. L. Rogach et al., “Lab-in-a-drop: controlled self-assembly of CdSe/ZnS quantum dots and quantum rods into polycrystalline nanostructures with desired optical properties,” *Nanotechnology*, vol. 18, no. 18, Article ID 185602, 2007.
- [59] A. Zalecka, *Development and validation of the capillary dynamolysis method for the discrimination of chosen foods deriving from differently managed cultivation systems*, Ph.D. thesis, University of Kassel, 2007.
- [60] M. O. Kokornaczyk, *Quality comparison of organic and conventional wheat by use of common and holistic methods of analysis*, Ph.D. thesis, University of Pisa, 2008.

This article should be cited as follows:

Maria Olga Kokornaczyk, Giovanni Dinelli, Ilaria Marotti, Stefano Benedettelli, Daniele Nani, and Lucietta Betti, “Self-Organized Crystallization Patterns from Evaporating Droplets of Common Wheat Grain Leakages as a Potential Tool for Quality Analysis,” *TheScientificWorldJOURNAL*, vol. 11, pp. 1712–1725, 2011.
